Starting Circuit Adapted to Stabilize HID Lamps and Reducing the Acoustic Resonances

Mario Ponce-Silva, *Senior Member, IEEE*, Juan A. Aqui-Tapia, Rene Osorio, and Ricardo E. Lozoya-Ponce

***Abstract*—This paper presents an igniter circuit for high-intensity-discharge (HID) lamps based on an inverter and a resonant tank that has been adapted to stabilize inductively an HID lamp by means of applying low-frequency quasi-square waveforms to voltage and current in the lamp in order to reduce the presence of the acoustic resonances. With the proposed improvement, the igniter circuit performs three different functions: 1) the lamp ignition; 2) the arc stabilization; and 3) the acoustic resonances reduction. This proposal allows the use of fewer components, and less energy processing is minimized, so the resulting ballast is cheaper and more efficient than other ballast that avoids the acoustic resonances when they are working with square waveforms in the lamp voltage and current. The circuit was validated experimentally by using a 70 W conventional high-pressure sodium lamp, which is operated with a frequency of 2 kHz. The results were an electrical efficiency of 94%, a crest factor in the lamp current of 1.41, and it was not observed the presence of acoustic resonances.**

***Index Terms*—Acoustic resonances and quasi-square waveform, electronic ballast, high-Intensity discharge (HID).**

I. Introduction

DESPITE the recent boom of power LEDs [1]–[5], which have been used in street lighting applications, the high-intensity-discharge (HID) lamps remain an attractive option due to their high efficiency, long useful life, and low cost. However, these kind of lamps are susceptible to the acoustic resonances phenomenon [6]–[8]. One of the solutions for this problem is to feed these lamps with low-frequency square waveforms in the lamp voltage and current [7]–[14], this is because to feed HID lamps with square waveforms is an effective way to avoid acoustic resonances. However, this method presents the inconvenience of needing a complex and expensive ballast with many stages, which causes low electrical efficiency [15]–[18].

Manuscript received March 4, 2018; revised June 10, 2018 and August 30, 2018; accepted October 29, 2018. Date of publication November 7, 2018; date of current version May 22, 2019. This research was funded by Tecnológico Nacional de México. Recommended for publication by Associate Editor W. Kaiser. *(Corresponding author: Mario Ponce-Silva.)*

M. Ponce-Silva is with the Electronics Department, National Center of Research and Technological Development – CENIDET, Cuernavaca 62490, México (e-mail:

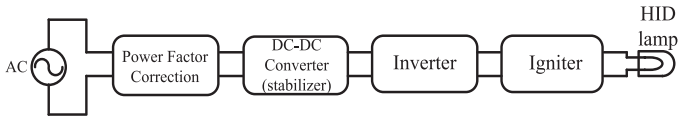

Fig. 1. Typical stages of a low-frequency square waveform ballast.

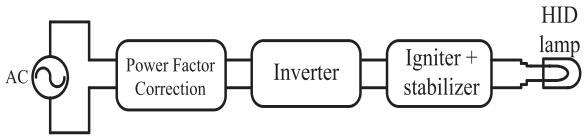

Fig. 2. Stages of a quasi-square waveform ballast.

Fig. 1 shows the stages of a typical square-waveform ballast, it consists of power factor correction circuit, dc–dc converter used to stabilize the arc discharge, an inverter, igniter, and the lamp [19]. In order to reduce the number of stages, an integration of some stages of the typical square waveform ballast in a single stage is proposed in this paper, this consists of the integration of the igniter stage and the dc–dc converter in a single stage in order to ignite, to stabilize the arc discharge, and to reduce the presence of the acoustic resonances in the lamp at the same time. The stabilization of the arc discharge is achieved by means of the inductance of the ignition circuit, and the acoustic resonances are minimized by applying low-frequency quasi-square waveforms in the voltage and the current of the lamp, which was presented in [20].

The diagram of the proposed ballast is shown in Fig. 2. As can be seen in this figure, the stabilization and the ignition stages are integrated into a single stage. The proposed integration eliminates one processing stage of the electrical energy, which allows a reduction in the energy processing increasing the electrical efficiency and reducing the number of components.

This paper is organized as follows. In Section II, the characteristic frequencies of the acoustic-resonances of the high-pressure sodium (HPS) lamp LU-70 from Lucalox were calculated. Based on this analysis, a relatively low switching frequency is proposed to reduce the presence of the acoustic resonances phenomenon. In Section III, the analysis of the proposed igniter plus the ballast circuit is presented. In Section IV, the prototype design is shown. In Section V, the experimental results are discussed; and, finally, in Section VI, the conclusions are presented.

II. Impact of the Acoustic Resonances in an HPS Lamp

To avoid the presence of acoustic resonances in HID lamps it is recommended that they must be operated in a range of

TABLE I
ACOUSTIC RESONANCE FREQUENCIES (kHz) FOR THE LAMP LUCALOX LU-70

F_{001}	F_{100}	F_{101}	F_{200}	F_{002}
5.63	153.3	153.4	254.4	11.26
F_{201}	F_{102}	F_{010}	F_{011}	F_{300}
254.2	153.7	319.3	319.4	350
F_{202}	F_{301}	F_{003}	F_{012}	F_{103}
254.4	350	16.89	319.5	154.3
F_{302}	F_{400}	F_{110}	F_{401}	F_{111}
350.2	443.1	444.3	443.2	444.3
F_{203}	F_{013}	F_{402}	F_{112}	F_{004}
254.7	319.8	443.2	444.4	22.52

where:
F_{100}= acoustic resonance frequency, azimuthal component.
F_{010}= acoustic resonance frequency, radial component.
F_{001}= acoustic resonance frequency, longitudinal component.

low frequencies (200–400 Hz), this is because this phenomenon does not appear at these frequencies.

To determine a proper operating frequency of the ballast, a theoretical analysis to find the eigen frequencies of the lamp Lucalox LU-70 is shown. This lamp has the following dimensions: tube discharge ratio equal to 3 mm, and a length of 44.4 mm. The calculation is done by using the following equation [6]:

$$f_{lmn} = \frac{C_s}{2}\sqrt{\left(\frac{n}{L}\right)^2 + \left(\frac{\alpha_{lm}}{R}\right)^2} \text{ with } n = 0, 1, 2 \ldots \quad (1)$$

where

f_{lmn} is the natural frequency of a cylindrical tube, at this frequency the acoustic resonances may appear and can be expressed in function of the angular frequency ω by $f_{lmn} = \omega/2\pi$;

C_s is the velocity of the sound, which propagates inside in the lamp ($500\frac{m}{s}$);

α_{lm}, is the m-esimo zero of J_1, which is the first derivate of the first-order Bessel function J_1;

R is the ratio of the arc tube;

n is the number of nodal circles;

L is the length of the arc tube.

Using the dimensions of the lamp and based on the analysis done in [21], Table I was obtained, which shows the values of the acoustic resonance power frequencies (longitudinal, radial, and azimuthal), in a range of 5–155 kHz frequencies.

The frequencies presented in Table I are related to the waveform of the lamp power. As can be seen, the lowest frequency for the eigen frequencies is $F_{001} = 5.63$ kHz. Therefore, according to this theoretical analysis, the appearance of acoustic resonances below this frequency is improbable. Therefore, the switching frequency was established at $f_s = 2$ kHz in order to avoid the presence of acoustic resonances in the lamp Lucalox LU-70, this condition do not guarantee the total elimination of the acoustic resonances, but the probability of their presence is significantly reduced. The effect of the impedance of the passive element is low at low frequencies (2 kHz), and the size of these elements is acceptable at 2 kHz.

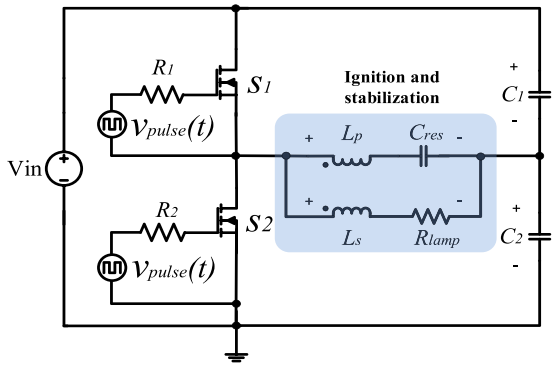

Fig. 3. Proposed electronic ballast.

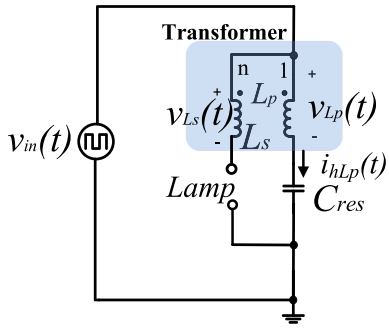

Fig. 4. Equivalent circuit of the proposed ballast during the ignition stage.

III. ANALYSIS OF THE PROPOSED BALLAST

As aforementioned in the introduction, the main contribution of this paper is the use of an igniter circuit not only to start the lamp, but also for stabilizing the arc discharge and for reducing the acoustic resonance phenomenon. The proposed ballast is shown in Fig. 3, it consists of a dc regulated voltage, which could be provided by a previous stage (power factor corrector). The dc voltage is supplied to a half-bridge inverter with a resonant igniter, which is formed by a transformer (L_p and L_S) and a capacitor (C_{res}). The magnetizing inductance of the primary inductor (L_p) is connected in series with the capacitor C_{res}, and the secondary inductor (L_s) is connected in series with the lamp.

The operation of the ballast has two states, which are described as follows.

1) *Ignition stage:* The equivalent circuit of the ballast during this stage is shown in Fig. 4, where $V_{\text{in}}(t)$ is the voltage that could be supplied by a power factor corrector. The half-bridge inverter operates at high frequency ($f_s \geq 100$ kHz), and its main function is to feed the igniter (the series connection of the resonant tank $L_p - C_{\text{res}}$) with square waveforms. If the resonant tank formed by $L_p - C_{\text{res}}$ is in resonance, a high current circulates through the resonant tank. This current produces a high voltage in the primary of the transformer formed by L_s and L_p. Therefore, due to the transformer operation, a high voltage is also applied to the lamp. The igniter provides,

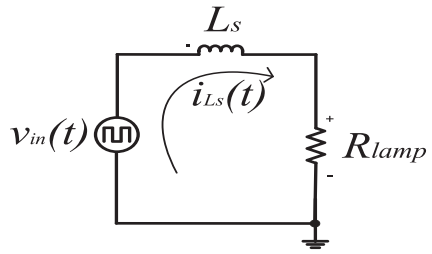

Fig. 5. Equivalent circuit during the steady-state stage.

for a short time, pulses of high voltage for the ignition of the lamp. The duration of this stage is about only 1–3 ms.

2) *Steady-state stage*: During this stage, the lamp is modeled as a constant resistance. The switching frequency of the inverter is changed to the minimum value ($f_s = f_{\text{low}} =$ 2 kHz), with the objective of increasing the impedance of the capacitor C_{res}, which causes the value of the lamp current to decrease. This current could be neglected with respect to the lamp current, so that the impedance of the capacitor could be considered high (open circuit). At the new switching frequency, the secondary winding of the transformer (L_s) limits the current through the lamp and apply a quasi-square waveform in the current and the voltage in the lamp. The equivalent circuit of the proposed ballast during this stage is shown in Fig. 5.

When the current in the resonant capacitor is almost zero with respect to the lamp current, the transformer (L_p and L_S) behaves like a simple inductor L_s.

A. Analysis of the Equivalent Circuit During the Steady-State Stage

To simplify the analysis of the circuit shown in Fig. 5, the following conditions are assumed.

1) The switches of the half-bridge inverter are considered as ideals.
2) The behavior of the lamps is like a constant resistance (R_{Lamp}).
3) The half-bridge inverter supplies a symmetrical square voltage waveform without death time and with a duty cycle D of 50%.

Under the previous conditions, the Kirchhoff voltage law can be used to analyze the circuit given in Fig. 1. The following differential equation is obtained:

$$L_s \frac{di_{L_s}(t)}{dt} + R_{\text{lamp}} i_{L_s}(t) - v_{\text{in}}(t) = 0 \tag{2}$$

where $V_{\text{in}}(t)$ is

$$v_{\text{in}}(t) = \begin{cases} V_{\text{in}} & 0 \le t < T/2 \\ 0 & T/2 \le t < T. \end{cases} \tag{3}$$

Equation (2) has the following solution:

$$i_{L_s}(t) = \begin{cases} \frac{V_{\text{in}}}{R_{\text{Lamp}}}\left[1 - e^{-\frac{t}{\tau}}\right] - I_0 e^{-\frac{t}{\tau}} & 0 \le t < \frac{T}{2} \\ \frac{-V_{\text{in}}}{R_{\text{Lamp}}}\left[1 - e^{-\frac{t}{\tau}}\right] + I_0 e^{-\frac{t}{\tau}} & \frac{T}{2} \le t < T \end{cases} \tag{4}$$

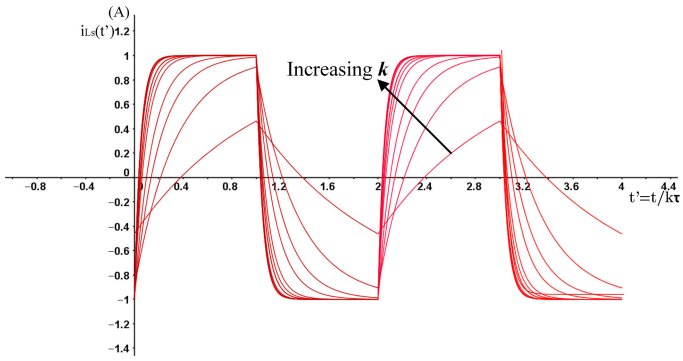

Fig. 6. Normalized current in the lamp $i_{Ls}(t)$ for several time constants (k).

where V_{in} is the maximum value of $v_{\text{in}}(t)$, T is the period at steady state, I_0 is the value of the current during the transition from positive to negative of the voltage $v_{\text{in}}(t)$ and it is the maximum value of the current $i_{LS}(t)$, therefore

$$I_0 = i_{Ls}\left(\frac{T}{2}\right). \tag{5}$$

τ is given by

$$\tau = \frac{L_{\text{s}}}{R_{\text{lamp}}}.$$

It is better to express the time as a function of the constant τ with the purpose of simplifying the expression of the current. Therefore, the half of the period is defined as follows:

$$\frac{T}{2} = k\tau \tag{6}$$

where k is a constant, the previous equation indicated that the half period is reached at k times of the constant τ.

Substituting (5) and (6) into (4), the following expression for I_0 is obtained:

$$I_0 = c\frac{V_{\text{in}}}{R_{\text{Lamp}}} \tag{7}$$

where the constant c is as follows:

$$c = \frac{1 - e^{-k}}{1 + e^{-k}}. \tag{8}$$

Normalizing the values of $V_{\text{in}} = 1, R_{\text{Lamp}} = 1$, and plotting in function of the time $t' = \frac{t}{k\tau}$, the plot shown in Fig. 6 was obtained.

Based on Fig. 6, the current $i_{Ls}(t)$ through the circuit has an exponential evolution and it tries to reach the value of $V_{\text{in}}/R_{\text{Lamp}}$. However, the current only will reach the value of $I_0 = 1$, which is the initial condition of the next stage. If $k \ge 5$ and $c \approx 1$ in (8), then $I_0 \approx V_{\text{in}}/R_{\text{Lamp}} = 1$. While the value of k continues to increase, the waveform of the lamp current is squarer.

If the lamp had a constant resistive behavior, then the voltage waveform in the lamp would be similar to the current waveform shown in Fig. 6. Therefore, the normalized instant power waveform $p(t) = v(t)i(t)$ will be proportional to $i_{Ls}(t)^2$ and will have the waveform shown in Fig. 7.

As can be seen in Fig. 7 for values of $k > 1$, the instant power in the lamp $p(t)$ becomes more constant, except for the

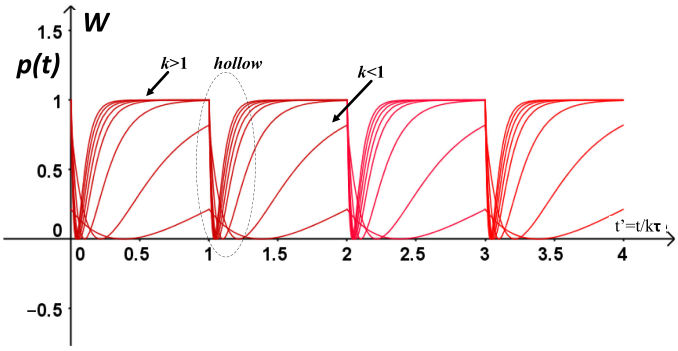

Fig. 7. Normalized instant power waveform delivery to the lamp $p(t)$ during the steady-state operation for several values of the constant k.

"hollow" corresponding to the zero crossing of the current and voltage waveforms in the lamp. Constant power in the lamp reduces the harmonic content, and the possibility of occurrence of the acoustic resonances is also reduced. Thus, to significantly reduce the presence of the acoustic resonances, it is important to consider that the following condition must be fulfilled: $k > 1$.

B. Power Delivered to the Lamp

Considering a constant resistive behavior of the lamp, the average power delivered to the lamp could be expressed as follows:

$$P = {I_{Ls\text{rms}}}^2 R_{\text{lamp}} \tag{9}$$

where $I_{Ls\text{rms}}$ is the RMS value of the current in the lamp $i_{Ls}(t)$. Since the current waveform is symmetric, then the term $I^2_{L\text{rms}}$ can be evaluated with the following expression:

$${I_{Ls\text{rms}}}^2 = \frac{2}{T}\int_0^{\frac{T}{2}} (I_{Ls}(t))^2 dt. \tag{10}$$

Substituting (4) in (10), the following equation is obtained:

$${I_{Ls\text{rms}}}^2 = \frac{2{V_{\text{in}}}^2}{T{R_{\text{lamp}}}^2}\left[\begin{array}{c} \frac{T}{2} + 2(1+c)\frac{L_s}{R_{\text{lamp}}}\left(e^{-\frac{T}{2\tau}} - 1\right) \\ -\frac{L_s}{2R_{\text{lamp}}}(1+c)^2\left(e^{-\frac{T}{\tau}} - 1\right) \end{array}\right]. \tag{11}$$

And substituting (6) in (11), the following equation is obtained:

$${I_{Ls\text{rms}}}^2 = \frac{{V_{\text{in}}}^2}{{R_{\text{lamp}}}^2}\left[\begin{array}{c} 1 + \frac{2(1+c)}{k}\left(e^{-k} - 1\right) \\ -\frac{1}{2k}(1+c)^2\left(e^{-2k} - 1\right) \end{array}\right]. \tag{12}$$

To simplify the analysis, a variable auxiliary $a = f(c.k)$, which is only in function of the constants c and k, is considered:

$$a = f(c,k) = \left[\frac{1}{2} + \frac{(1+c)}{k}\left(e^{-k} - 1\right) - \frac{1}{4k}(1+c)^2\left(e^{-2k} - 1\right)\right]. \tag{13}$$

Therefore

$${I_{Ls\text{rms}}}^2 = \frac{{V_{\text{in}}}^2}{{R_{\text{lamp}}}^2}[a]. \tag{14}$$

An expression for the value of V_{in} can be obtained by substituting (14) into (9) as follows:

$$P = \frac{{V_{\text{in}}}^2 a}{R_{\text{Lamp}}} \rightarrow V_{\text{in}} = \frac{\sqrt{R_{\text{Lamp}}P}}{\sqrt{a}}. \tag{15}$$

The inductor L_s can be calculated by using (6)

$$L_s = \frac{R_{\text{Lamp}}T}{2k} = \frac{R_{\text{Lamp}}}{2kf_{\text{low}}} \tag{16}$$

where f_{low} is the switching frequency of the half-bridge inverter during the steady-state operation.

C. Analysis of the Starter Circuit

The equivalent circuit during the ignition stage is shown in Fig. 4, as can be seen in this figure, the lamp behaves like an open circuit, and the transformer behaves like a single inductor L_p, this inductor represents the self-inductance of the transformer, which is the sum of the magnetizing inductance (L_{mp}) and the leakage inductance (L_{lp}) of the transformer primary. The starting circuit is designed with the aim that the switching frequency during this stage ($f_{s\text{high}}$) be very close to the resonant frequency of the resonant tank formed by the self-inductance L_p and the capacitor C_{res}. Thus, the current through the resonant circuit will be large, which produces a high voltage across the transformer primary $v_{Lp}(t)$. In the secondary side of the transformer, this voltage will rise further due to the turns ratio of the transformer $v_{Ls}(t) = n\, v_{Lp}(t)$, which causes the turn-on of the lamp. Once the lamp is turned on, the switching frequency is changed from the starting frequency ($f_{s\text{high}} = 150\,\text{kHz}$) to the minimum frequency ($f_{\text{slow}} = 2\,\text{kHz}$) for the steady-state operation. The ignition state occurs in a short time, in the order of milliseconds. Nevertheless, it is important to limit the current in the primary side of the transformer to prevent its saturation.

The analysis of the circuit of Fig. 4 can be done by considering only the fundamental component of the lamp voltage. Therefore, the following assumptions must be considered in the analysis.

1) For the ignition stage, the switching frequency ($f_s = f_{\text{high}}$) is very high compared with the steady-state switching frequency ($f_s = f_{\text{low}}$), $f_{\text{high}} \gg f_{\text{low}}$.
2) The quality factor (Q) of the circuit during the ignition state is very high, $Q \gg 1$. Therefore, the current through the inductor L_p and the capacitor C_{res} is almost sinusoidal.
3) The starting circuit must be deactivated automatically after the turn-on of the lamp. Therefore, the switching frequency ($f_s = f_{\text{low}}$) must have a value such as the reactance ($X_l = X_{lLp} - X_{lC\text{res}}$) formed by the self-inductance L_p (X_{lLp}) of the primary and the impedance of the resonant capacitor C_{res} (X_{lCres}) be much greater than the impedance ($Z = \sqrt{{X_{lLs}}^2 + R^2_{\text{Lamp}}}$) formed by the self-inductance L_s (X_{lLs}) of the transformer secondary and the equivalent resistance of the lamp (R_{lamp}). So that the reactance X_l behaves as an open circuit compared with the impedance Z, this condition is accomplished if $f_{\text{high}} \gg f_{\text{low}}$.

TABLE II
SPECIFICATIONS FOR THE ANALYSIS OF THE IGNITION STATE

Symbol	Description
V_{in1}	Fundamental component of $V_{in}(t)$
I_{hp}	Peak value of the current in the side primary of the transformer, I_{hp}=Max[$i_{hLp}(t)$]
V_{st}	Suggested voltage to ignite the lamp
f_{high}	Switching frequency
ω_h	Angular frequency, $\omega_h = 2\pi f_{high}$
X_{hLp}	Reactance of L_p during this state. $X_{hLp} = \omega_h L_p$
X_{hCres}	Reactance of C_{res} during this state. $X_{hCres} = 1/(\omega_h C_{res})$
X_h	Equivalent reactance of the resonant tank formed by L_p and C_{res}. $X_h = X_{hLp}$- X_{hCres}

For the steady-state analysis of the circuit shown in Fig. 4 ($f_s = f_{\text{high}}$), the following specifications are defined (see Table II).

From (3)

$$V_{\text{in1}} = \frac{2V_{\text{in}}}{\pi}. \tag{17}$$

The maximum voltage in L_p is given by the following:

$$V_{Lp} = V_{\text{in1}} \frac{X_{hLp}}{X_h}. \tag{18}$$

If $\frac{V_{Ls}}{V_{Lp}} = n$, $\frac{Ls}{Lp} = n^2$, then

$$V_{st} \approx V_{Ls} = \frac{I_{hp} X_{hLs}}{n} \tag{1}$$

$$n = \frac{I_{hp}\omega_h L_s}{V_{st}}. \tag{19}$$

From Fig. 4

$$X_h = \frac{V_{\text{in1}}}{I_{hp}}. \tag{20}$$

Substituting (17) into (20), the following equation is obtained:

$$X_{hCrs} = X_{hLp} - \frac{2V_{\text{in}}}{\pi I_{hp}}. \tag{21}$$

IV. DESIGN OF THE PROPOSED BALLAST

According to the analysis performed in the steady and ignition states, the design equations were obtained, shown in Table III, which presents the design methodology of the *Lamp LU-70 from Lucalox company*.

The design was done for a half-bridge inverter with the following data: $k = 5$, $R_{\text{lamp}} = 77\,\Omega$, $P_{\text{lamp}} = 70\,\text{W}$, $f_{\text{low}} = 2\,\text{kHz}$, $V_{st} = 6\,\text{kV}$, $I_{hp} = 15\,\text{A}$ and $f_{\text{high}} = 150\,\text{kHz}$.

V. EXPERIMENTAL RESULTS

To validate the performance of the proposed ballast, a prototype was implemented. The transformer was designed using the geometric constant K_g method [21]. The transformer was considered as two coupled inductors, each inductor was designed separately. A maximum current of 20 A in the primary inductor was proposed to assess the total gap and to avoid the core saturation. First, it was obtained the *Kg* constant for each inductor (*KgLs* and *KgLp*) to obtain the total *KgT* total as the sum of both *KgLs* and *KgLp* constants of each inductor. The selected core and material were the ETD39-3C85. To minimize the skin effect, a braided wire was used, for the primary inductor, 19 braided wires of AWG #30 was considered, and for the secondary inductor only 1 wire with AWG #24 was used.

TABLE III
DESIGN METHODOLOGY

Parameter	Equation	Calculated value
c	$\frac{1-e^{-k}}{1+e^{-k}}$	0.986
a	$\left[\frac{1}{2}+\frac{(1+c)}{k}\left(e^{-k}-1\right)-\frac{1}{4k}(1+c)^2\left(e^{-2k}-1\right)\right]$	0.6053
V_{in}	$\frac{\sqrt{R_{lamp}P_{lamp}}}{\sqrt{a}}$	188.6 V
τ	$\frac{1}{2kf_{low}}$	50 µ
L_s	τR_{lamp}	3.85 mH
$I_{L_s rms}$	$\sqrt{\frac{P_{lamp}}{R_{lamp}}}$	0.95 A
n	$n = \frac{I_{hp}\omega_h L_s}{V_{st}}$	9
L_p	$\frac{Ls}{n^2}$	46.8µH
C_{res}	$\frac{1}{\omega_h X_{hCrs}}$	29.4nF

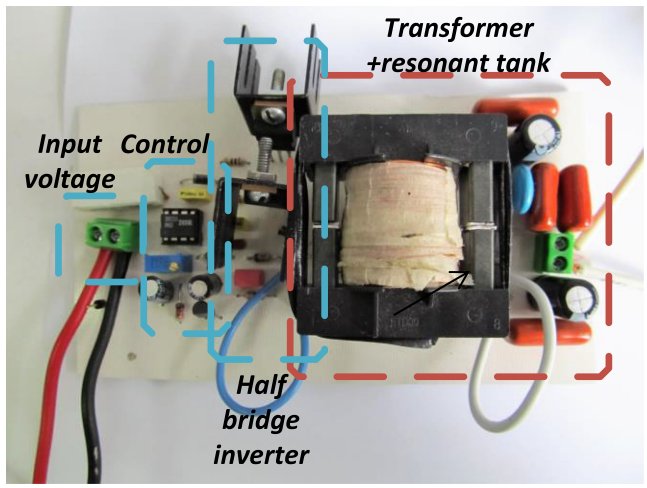

Fig. 8. Implemented prototype.

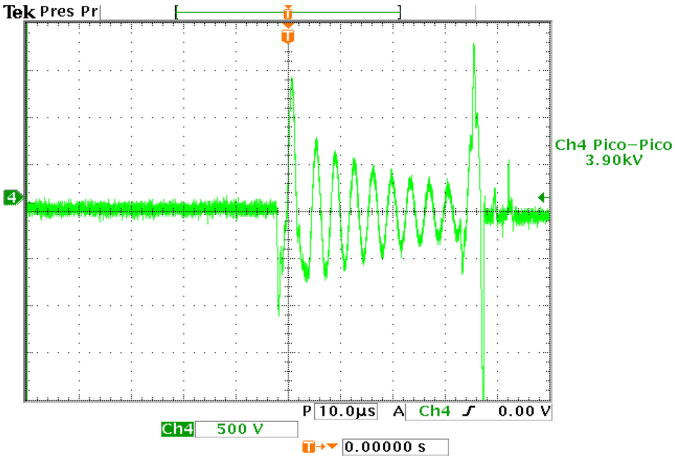

Fig. 9. Voltage on the lamp during the ignition state. Vertical: 500 V/div, horizontal: 10 μs/div.

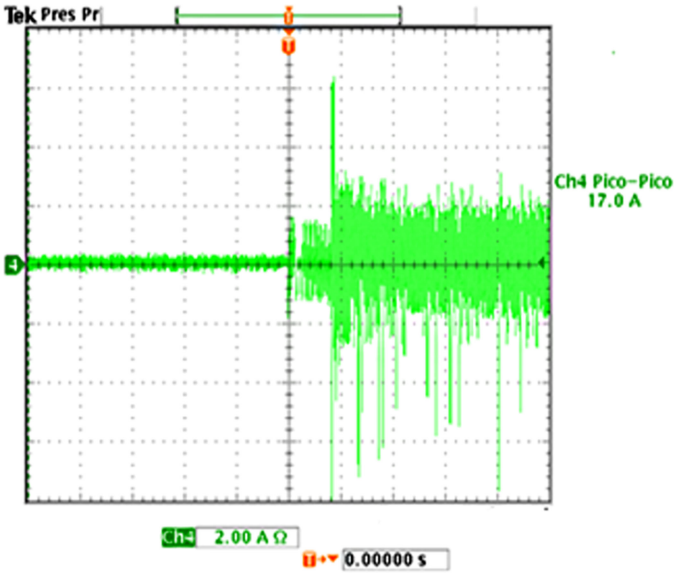

Fig. 10. Current in the lamp during the ignition state. Vertical: 2 A/div, horizontal: 40 μs/div.

Fig. 8 shows the implemented prototype, where the transformer, control circuit, and half-bridge plus resonant tank are shown.

The MOSFETs used were IRF640s and the driver was the IR2153. Also, for the measurements, an oscilloscope Tektronix TDS3054B with the probes P6015A, TCP202, P5210A and P2220 was used. In the next sections, the results in both operation conditions, ignition, and steady-state operation are presented.

A. Ignition State Results

Fig. 9 shows the plot of the lamp voltage. In this figure, a peak-to-peak voltage of 3.9 kV is observed, which occurs before the steady-state operation.

Fig. 10 shows the current on the lamp during the ignition state, where a peak-to-peak current of 17 A is observed.

The theoretical ignition voltage and current previously proposed and the real values obtained in the experimental results

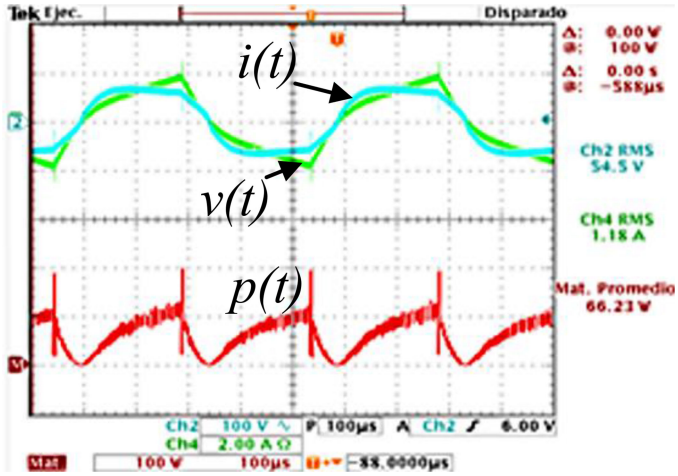

Fig. 11. Voltage, $v_{\text{lamp}}(t)$ 100 V/div, current, $i_{\text{lamp}}(t)$ 2 A/div, and power, $P_{\text{lamp}}(t)$ 100 W/div, in the lamp. Horizontal scale: 100 μs/div.

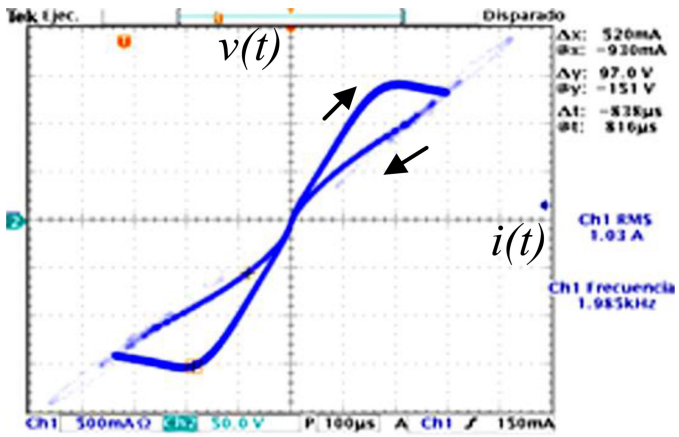

Fig. 12. Current versus voltage in the lamp. Vertical: 50 V/div, horizontal: 500 mA/div.

are not exactly the same because there are parasitic elements in the transformer and in the resonant capacitor. However, the ignition voltage obtained in the experimental prototype was enough to turn-ON the lamp.

B. Steady-State Results

In Fig. 11 are shown the instant current, the voltage, and the power in the lamp during the steady-state operation. These waveforms are similar to a quasi-square waveform in the lamp, which is shown in Figs. 6 and 7, the difference between both is caused by the non-linear behavior of the lamp.

In Fig. 12 is observed the instant current versus the voltage in the lamp. According to these graphics, it was concluded that the lamp does not present a resistive behavior (linear behavior), because of this, the current and voltage waveforms are not completely square.

In Fig. 13, the current, voltage, and power signals in one MOSFET are shown, according to these plots there is a loss of 0.2012 W in each MOSFET.

Fig. 14 shows the harmonic content of the lamp power. The value of the magnitude of each component is obtained through

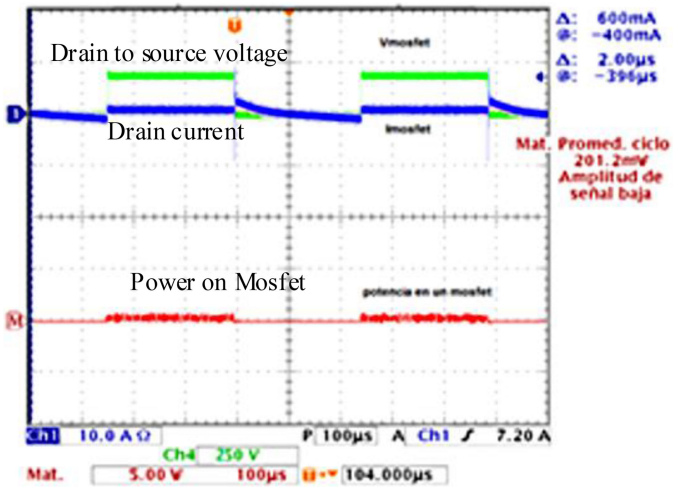

Fig. 13. Drain to source voltage 250 V/div, drain current 10 A/div and instant dissipated power 5 W/div in one MOSFET.

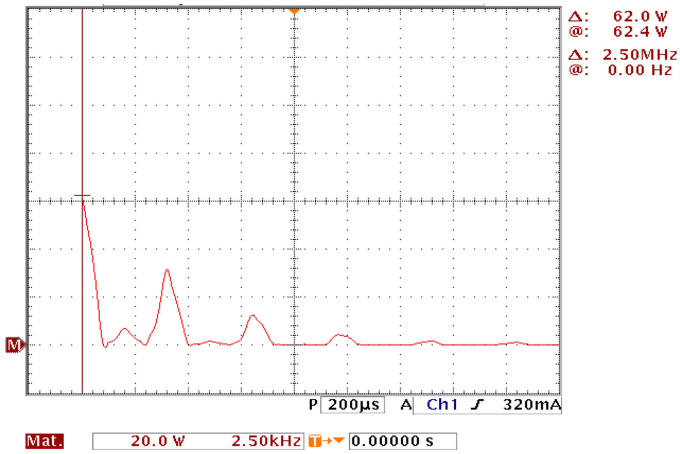

Fig. 14. Instant power harmonics in the lamp. Horizontal: 20 W/div, vertical: 2.5 kHz/div.

TABLE IV
HARMONIC CONTENT OF THE LAMP POWER

Harmonic number	Frequency (kHz)	Power (W)
1	0	62.4
2	2	9
3	4	32
4	8	13
5	12	4.5
6	16	2
7	20	1.15

the oscilloscope cursor. As can be seen in this figure, the amplitude of the harmonics is reduced when the frequency of each harmonic goes higher. Therefore, the probability to excite acoustic resonances presented above of 5 kHz is lower.

In Table IV is shown the frequency of each harmonic and its amplitude. According to this table, the power supplied to the lamp by the fifth harmonic is very small compared with the power supplied by the fundamental. Therefore, it can be said that the probability of the other higher frequency harmonics which excite the acoustic resonances is very low.

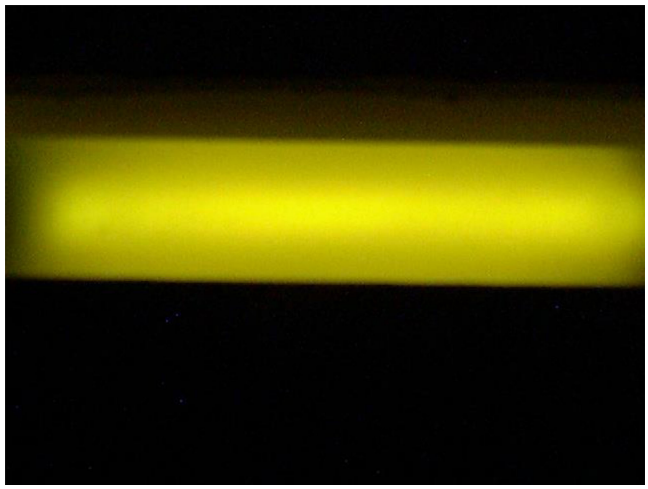

Fig. 15. Arc discharge of the lamp LU-70 fed with the proposed ballast.

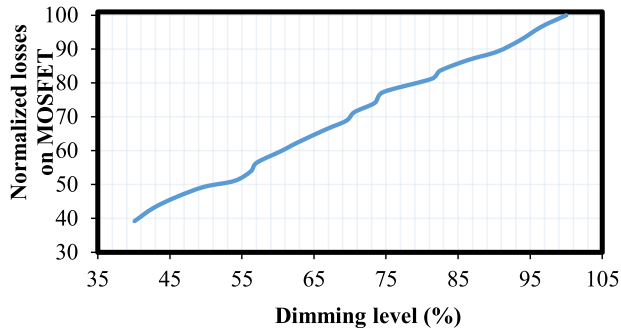

Fig. 16. Normalized losses in the MOSFET vs. dimming level.

To verify the absence or presence of acoustic resonances in the discharge arc of the lamp, a photograph of the form of the arc discharge operated with the proposed ballast is shown in Fig. 15. As can be observed in Fig. 15, the form of the arc is straight, therefore, for this lamp and for this test, the acoustic resonances were not observed.

C. Experimental Behavior of the Ballast With Dimming

In this section, the performance of the ballast with dimming is presented. The observed variables are the losses in the MOSFET, the electrical efficiency, and the crest factor.

Fig. 16 shows the losses in one MOSFET when a dimming test is performed, these results are normalized. According to this figure, the losses are reduced up to 40% at the lowest dimming level.

Fig. 17 shows the efficiency of the ballast versus the dimming level; the efficiency varies between 93% and 95% when the dimming level varies from 50% to 100%. As can be seen in this plot, the efficiency has little variations. The lower efficiency (87.7%) was obtained with a dimming level of 39%.

Fig. 18 shows the crest factor in the lamp current versus the dimming level. As can be seen in this plot, the crest factor does not present a significant variation during the dimming test. The crest factor affects the lifespan of the lamp. At the nominal power, the crest factor is about 1.41, which is the same value

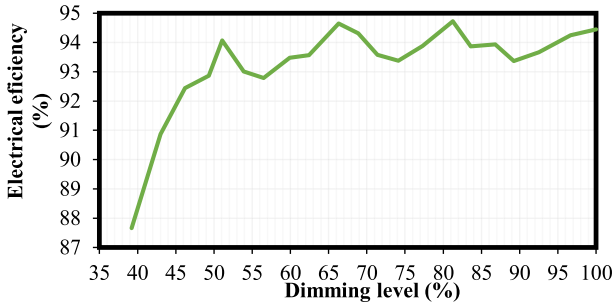

Fig. 17. Electrical efficiency vs. dimming level.

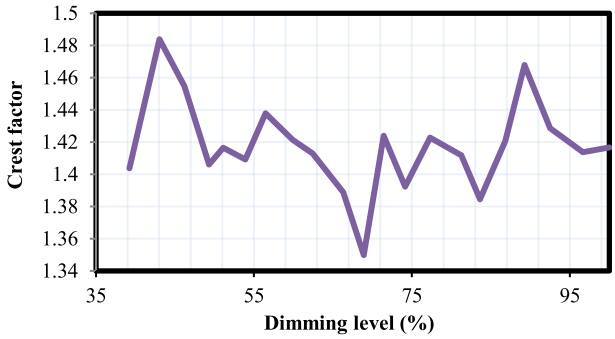

Fig. 18. Crest factor vs. dimming level.

for the sinusoidal waveforms obtained with a typical resonant electronic ballast [22].

VI. Conclusion

Power LEDs are increasing their presence in street lighting applications. However, HID lamps, and specifically, sodium vapor lamps continue to be a good option and are being used in many cities. This paper presents a ballast for HID lamps, whose principal contribution is to be used in a very simple and cheap resonant tank to ignite, to stabilize, and to significantly reduce the presence of the acoustic resonances by applying quasi-square waveforms in the lamp voltage and the current. An HPS lamp is fed with this kind of waveforms at a low frequency of 2 kHz, these conditions cause a reduction in the amplitude of the higher frequencies power harmonics and no acoustic resonances were observed in the tested lamp.

The proposed ballast was implemented, and the theoretical calculus was validated experimentally. The designed resonant tank achieves to ignite, to stabilize, and to reduce acoustic resonances in a high-pressure sodium vapor lamp. The resonant tank integrates the stabilizer and igniter circuit in one stage obtaining an efficiency of 94%; the ballast does not require protection for the absence of lamp. Finally, the proposed topology and the presented design methodology can be used to drive other discharge lamps.

References

[1] W. Yijie, G. Yueshi, R. Kailin, W. Wei, and X. Dianguo, "A single-stage LED driver based on BCM boost circuit and LLC converter for street lighting system," *IEEE Trans. Ind. Electron.*, vol. 62, no. 9, pp. 5446–5457, Sep. 2015.

[2] P. Santos Almeida, D. Camponogara, M. Dalla Costa, H. Braga, and J. M. Alonso, "Matching LED and driver life spans: A review of different techniques," *IEEE Ind. Electron. Mag.*, vol. 9, no. 2, pp. 36–47, Jun. 2015.

[3] J. C. W. Lam and P. K. Jain, "A high power factor, electrolytic capacitorless AC-input LED driver topology with high frequency pulsating output current," *IEEE Trans. Power Electron.*, vol. 30, pp. 943–955, 2015.

[4] A. Farahat, A. Florea, J. L. Martinez Lastra, C. Branas, and F. J. Azcondo Sanchez, "Energy efficiency considerations for LED-based lighting of multipurpose outdoor environments," *IEEE J. Emerg. Sel. Topics Power Electron.*, vol. 3, no. 3, pp. 599–608, Sep. 2015.

[5] C. Chun-An, C. Chien-Hsuan, C. Tsung-Yuan, and Y. Fu-Li, "Design and implementation of a single-stage driver for supplying an LED street-lighting module with power factor corrections," *IEEE Trans. Power Electron.*, vol. 30, no. 2, pp. 956–966, Feb. 2015.

[6] J. J. de Groot and J. A. J. M. van Vliet, *The High-Pressure Sodium Lamp*. New York. NY, USA: MacMillan, 1986.

[7] C. Hung-Liang and W. Ping-Wen, "A novel single-stage high-power-factor electronic ballast for metal-halide lamps free of acoustic resonance," *IEEE Trans. Power Electron.*, vol. 26, no. 5, pp. 1480–1488, May 2011.

[8] C. Chun-An, C. Hung-Liang, K. Chen-Wei, and C. Tsung-Yuan, "Design and implementation of a single-stage acoustic-resonance-free HID lamp ballast with PFC," *IEEE Trans. Power Electron.*, vol. 29, no. 4, pp. 1966–1976, Apr. 2014.

[9] C. A. Cheng, K. J. Lin, and Y. M. Kao, "Acoustic-resonance-free electronic ballast for automotive HID lamps," *Electron. Lett.*, vol. 44, pp. 1027–1029, 2008.

[10] C. Chun-An, C. Hung-Liang, C. Kuan-Lin, L. Kun-Jheng, and W. Ping-Wen, "A compact, high-power-factor HID lamp ballast," in *Proc. Int. Conf. Power Electron. Drive Syst.*, 2009, pp. 967–972.

[11] E. Enriquez, M. Ponce-Silva, M. Cotorogea, R. Osorio, and M. Alonso, "HID lamps fed with square-waveforms: Dimming and frequency effects on stability, current-crest-factor and power-factor," *IEEE Trans. Ind. Appl.*, vol. 46, no. 4, pp. 1667–1673, Jul./Aug. 2010.

[12] M. A. Dalla Costa, A. L. Kirsten, J. M. Alonso, J. Garcia, and D. Gacio, "Analysis, design, and experimentation of a closed-loop metal halide lamp electronic ballast," *IEEE Trans. Ind. Appl.*, vol. 48, no. 1, pp. 28–36, Jan./Feb. 2012.

[13] D. Pappis, A. C. Schittler, J. R. Pause, M. A. D. Costa, A. Campos, and J. M. Alonso, "Modified flyback for HID supply: Design, modeling and control," in *Proc. IEEE Ind. Appl. Soc. Annu. Meeting*, 2011, pp. 1–8.

[14] C. Chun-An, C. Hung-Liang, C. Tsung-Yuan, and K. Chen-Wei, "Single-stage high-power-factor low-frequency square-wave-driven high-intensity-discharge lamp ballast," *IET Power Electron.*, vol. 6, pp. 672–682, 2013.

[15] H. Chien-Ming, L. Tsorng-Juu, L. Ray-Lee, and C. Jiann-Fuh, "A novel constant power control circuit for HID electronic ballast," *IEEE Trans. Power Electron.*, vol. 22, no. 5, pp. 1573–1582, Sep. 2007.

[16] L. Tsorng-Juu, C.-M. Huang, and C. Jiann-Fuh, "Two-stage high-power-factor electronic ballast for metal-halide lamps," *IEEE Trans. Power Electron.*, vol. 24, no. 12, pp. 2959–2966, Dec. 2009.

[17] C. Hung-Liang, M. Chin-Sien, Y. Chung-Sheng, and H. Chun-Kai, "Analysis and implementation of an HPF electronic ballast for HID lamps with LFSW voltage," *IEEE Trans. Power Electron.*, vol. 27, no. 11, pp. 4584–4593, Nov. 2012.

[18] L. Tsorng-Juu and C.-M. Huang, "Interleaving controlled three-leg electronic ballast for dual-HID-lamps," *IEEE Trans. Power Electron.*, vol. 23, no. 3, pp. 1401–1409, May 2008.

[19] M. A. Dalla-Costa, J. M. Alonso, J. C. Miranda, J. Garcia, and D. G. Lamar, "A single-stage high-power-factor electronic ballast based on integrated buck flyback converter to supply metal halide lamps," *IEEE Trans. Ind. Electron.*, vol. 55, no. 3, pp. 1112–1122, Mar. 2008.

[20] J. M. A. O. Vila-Masot, "Low frecuency square wave electronic ballast for gas discharge," U.S. Patent 5428268, 1995.

[21] R. W. Erickson and D. Maksimovic, *Fundamentals of Power Electronics*. New York, NY, USA: Springer, 2007.

[22] A. Shrivastava and B. Singh, "Improved power quality converter based electronic ballast with high power factor," in *Proc. IEEE 5th India Int. Conf. Power Electron.*, 2012, pp. 1–6.

Authors' photograph and biography not available at the time of publication.